Published in IET Optoelectronics
Received on 28th November 2007
Revised on 15th February 2008
doi: 10.1049/iet-opt:20070084

Special Issue – Selected papers from NPL's Optical Fibre Measurement Conference (OFMC) 2007

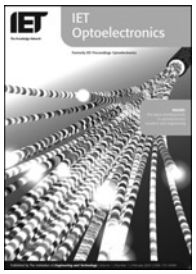

ISSN 1751-8768

# Mode control for emerging link performance standards

*A.G. Hallam*[1,2] *D.A. Robinson*[3] *I. Bennion*[1]

[1]*The Photonics Research Group, Aston University, Birmingham B4 7ET, UK*
[2]*'Sandridge', Winchester Road, Waltham Chase, Hampshire SO32 2LG, UK*
[3]*Arden Photonics Ltd, iBIC, Holt Court Road, Aston Science Park, Birmingham B7 4EJ, UK*
*E-mail: ahallam@halcyon-optical.co.uk*

**Abstract:** A novel mode control device is described, comprising a point-load mode scrambler in tandem with a mode filter. The device may be tuned to ensure compliance of fibre test equipment with new link performance standards. Improvement in the reproducibility of insertion loss measurements on concatenated fibres is demonstrated.

## 1 Introduction

Emerging standards for 1 and 10 Gb/s Ethernet transmission over multimode optical fibre have led to a resurgence of interest in the precise control and specification of modal launch conditions. In particular, ISO/IEC14763-3 [1] and IEEE802.3 [2] specify modal launch in terms of the mode power distribution (MPD) [3] and encircled flux [4], respectively. Commercial LED and optical time domain reflectometry (OTDR) test equipment does not, in general, comply with these standards and so there is a need for mode control devices to enable test sets to comply with the standards. A novel mode control device, comprising a mode scrambler operating in tandem with a mode filter, is described. An example of the improvement in loss measurements, resulting from the use of this device, is demonstrated by measuring the insertion loss of a series of concatenated patchcords with a range of different launch conditions.

## 2 Mode scramblers

A variety of mode-scrambling techniques have been described in the literature, such as sinusoidal bending [5], devitrification [6] and microbending [7], applied to step-index fibres, and long period gratings (LPGs) [8], etched fibre ends [9] and offset launch [10], applied to graded-index fibres. In the case of a step-index mode scrambler, it is necessary to provide some additional mode filtering in the target graded-index fibre to achieve the required modal filling. There is an advantage therefore in providing the required amount of mode conditioning directly to the graded-index fibre and there are devices in the market designed to do this, which work by mechanically impressing an LPG on the fibre. To test this method, an LPG was constructed consisting of a bed of seven contacting pins, each of 1 mm diameter. A 50 μm graded-index fibre was positioned across the pins and pressed against them with a soft former, causing the fibre to take up the period of the grating. The fibre was illuminated with light at 850 nm from a single-mode fibre and the output intensity distribution was measured using a video microscope. The normalised near-field profiles, shown in Fig. 1, show that light was progressively coupled to higher-order modes, characterised by increased width of the near field, as the grating load was increased from 0 to 9 N. The distribution did not, however, approach that corresponding to the roughly triangular shape, corresponding to an equilibrium mode distribution [11], or to a parabolic shape, corresponding to a fully filled distribution. The reason for this is that the difference in propagation constant $\Delta\beta$ between all adjacent mode groups in a graded-index fibre is constant, so the LPG progressively couples light from the lowest-order modes to the higher-order modes and eventually to leaky and radiative modes, resulting in a squarish distribution. This device is thus not suitable for producing the finely tuned mode distributions that are required for the new standards. The approach taken here is therefore to apply a combination of a mode scrambler in

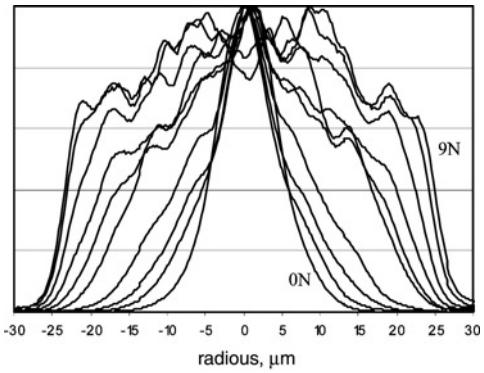


**Figure 1** *Near-field profiles of a 50 μm graded-index fibre in an LPG as the grating load was increased from 0 to 9 N*

series with a mode filter to enable flexibility and tuning of the modal distribution.

The newly proposed mode scrambler consists of bending a fibre round in a loop such that it crosses back over itself and applying a load to the crossover point. In this manner, each fibre section acts as a source of point loading for the other. The resultant distortion to the fibre leads to a wide spectrum of spatial frequencies in the fibre. This is a particular advantage for mode coupling in step-index fibres, where adjacent modes are not evenly spaced. For example, in a typical 50 μm step-index fibre at 850 nm, the difference in $\Delta\beta$ between adjacent modes varies from $1.5 \times 10^{-3}$ to 2.5 rad/mm. In contrast, for a 50 μm graded-index fibre, the 19 possible mode groups, each consisting of a number of degenerate modes, have almost identical spacing at 5.9 rad/mm.

The crossover point is sandwiched between two jaws of elastic material, shown in Fig. 2, such that application of a compressive force to the structure causes fibre sections A and B to be pressed into the jaws. A particular feature of this device is that it can be tuned in real time by adjusting the applied force while monitoring the output of the fibre. A further advantage is that point loading is applied equally to the fibre at two longitudinal positions, one loop-length apart, leading to a more complete mode scrambling. The distortion of the fibre may be calculated using bending beam theory as follows. From Roark [12], the displacement $y(z)$ of a concentrated load $W$ applied to an infinite beam on an elastic foundation, as a function of axial distance $z$, is

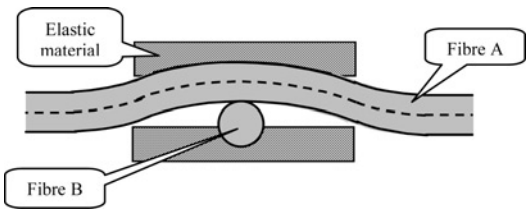


**Figure 2** *Schematic of crossover in point-load mode scrambler with silica fibre and elastic compression jaws*

given by

$$y(z) = -\frac{w}{8EI\phi^3} e^{-\phi z}(\cos \phi z + \sin \phi z) \quad (1)$$

where

$$\phi = \left(\frac{b_o k_o}{4ei}\right)^{1/4} \quad (2)$$

and $E$, $I$ and $b_o$ are Young's modulus, the moment of inertia and the width of the beam, respectively, and $k_o$ the foundation modulus (unit stress per unit deflection) [13]. The displacement of each individual fibre is equal to one-half of the displacement calculated from (1), as both jaws are compressed equally.

It is known [14] that the coupling strength between modes is proportional to the curvature spectrum of the fibre. The local fibre curvature $c(z)$ is given by [15]

$$c(z) = \frac{y''(z)}{\left(1 + y'(z)^2\right)^{3/2}} \quad (3)$$

For a given fibre, the shape of the curvature spectrum depends on the Young's moduli of the fibre and the jaw materials, and its amplitude depends on the applied load. Thus, selection of the jaw material, and the applied load, can be used to achieve a high degree of tuning.

As an example, consider a dual-coated silica fibre with Young's modulus values of 72 GPa, 10 MPa and 1.3 GPa for the cladding, inner coating and outer coating, respectively. Taking an area-weighted mean of the three materials gives an average Young's modulus of 18 GPa. Choosing, for example, polypropylene with Young's modulus 1.3 GPa, for the jaw material, and a load of 5 N, the curvature spectrum from (3) is shown in Fig. 3*a*. Also shown is a histogram of the frequency spectrum for coupling between adjacent fibre modes for a step-index fibre and a graded-index fibre. It can be seen that there is a significant overlap between the curvature spectrum and the spectrum of the graded-index fibre, but much less for the step-index fibre. Fig. 3*b* shows the respective spectra for coupling between all the modes, both adjacent and non-adjacent. Here, there is a high degree of overlap for the step-index fibre, indicating that the device should provide a high degree of mode scrambling for this type of fibre.

A practical implementation of the loop mode scrambler was constructed by forming a loop in the fibre and passing the end back through the loop. In this way, a stable loop of ~20 mm diameter could be formed. In this configuration, there are three crossover points situated in close proximity. The crossover points were located between two rigid jaws, each lined with a 400 μm thick film of polypropylene, and a compressive force was applied. The near-field intensity



doi: 10.1049/iet-opt:20070084

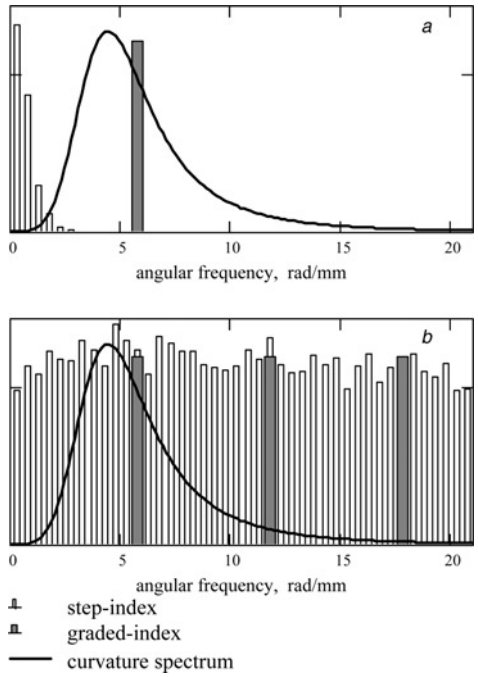


**Figure 3** *Curvature spectrum of point-load mode-scrambler, and $\Delta\beta$ spectrum for coupling between modes in step and graded-index fibres*

*a* Adjacent modes
*b* All modes

profiles at the output of the mode scrambler were measured as a function of applied load for an underfilled launch, shown in Fig. 4. It was found that even for zero loading there was a degree of natural mode scrambling occurring. The flat-topped profile occurring at 4 N indicated that the fibre modes were all equally excited. Increasing the load further caused a slight bias towards higher-order and leaky modes, identified by the concave shape. Note that, for clarity, the curves have been normalised and offset vertically. The output of the point-load device was then spliced to a 50 μm graded-index output fibre and the MPD was measured. The results, plotted in Fig. 5, show that for zero loading a single-mode launch clearly underfills the graded-index fibre. The MPD was computed using the measured refractive index profile of the fibre as the reference profile [3], and so a fully filled distribution would correspond to a diagonal line from the lower left to the top right corner. When a load of 6 N was applied, however, the MPDs for both launches converge to give a stable, fully filled, mode distribution.

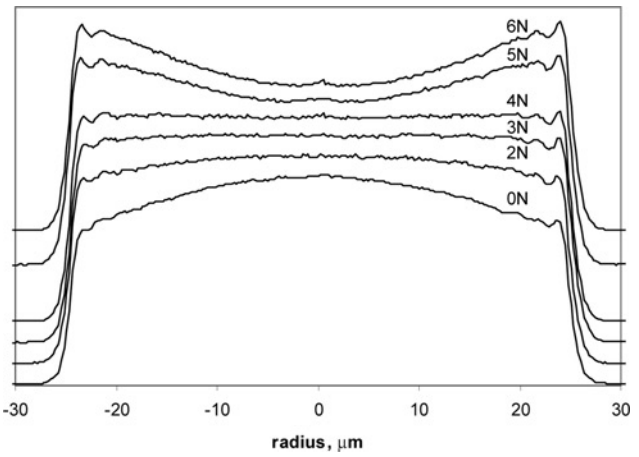


**Figure 4** *Near-field profiles of 50 μm step-index fibre against point loading*

## 3 Mode filters

In order to tune the mode distribution, the mode scrambler was tested in series with two types of mode filter, a longitudinal gap filter and a mandrel-wrap filter. The longitudinal gap filter consisted of a small air gap between two sections of step-index fibre, positioned immediately after the mode scrambler. The principle of the filter is that overlap of the higher-order modes from the source fibre with the target fibre becomes progressively less as the gap is increased. Fig. 6*a* shows a series of mode transfer function (MTF) curves as the gap is increased from 0 to 500 μm. For zero gap in the filter, the MTF is essentially of unity value for all modes, indicating a fully filled distribution. As the gap is increased, the MTF is attenuated in a manner roughly proportional to the mode group number.

The mandrel-wrap mode filter consisted of a single loop in the graded-index fibre around a mandrel. Fig. 6*b* shows the MTFs for a range of mandrel diameters, from essentially straight, down to 5 mm. For this filter, the MTF remained effectively unity up to a 'knee' position, where a roll-off in the higher mode groups occurred. The position of the knee shifted to the left, as the mandrel diameter was reduced. The corresponding encircled flux plots for these filters are shown in Fig. 7. As the gap in the air-gap filter is increased, the curves become steeper around the mid-radius

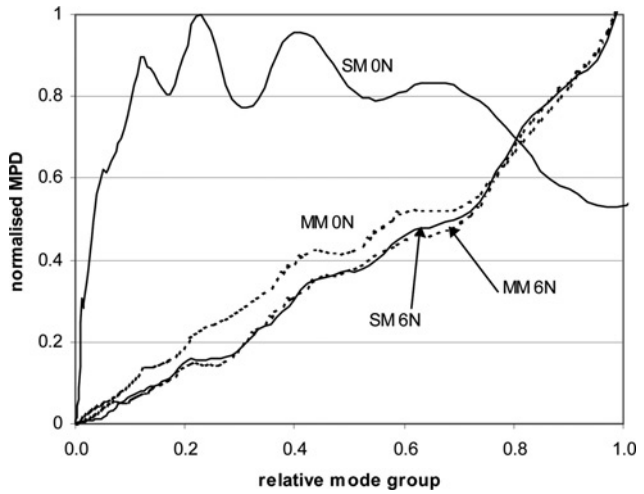


**Figure 5** *Measured MPDs of graded-index fibre spliced to point-load mode-scrambler, for singlemode (solid) and multimode (dotted) launches*

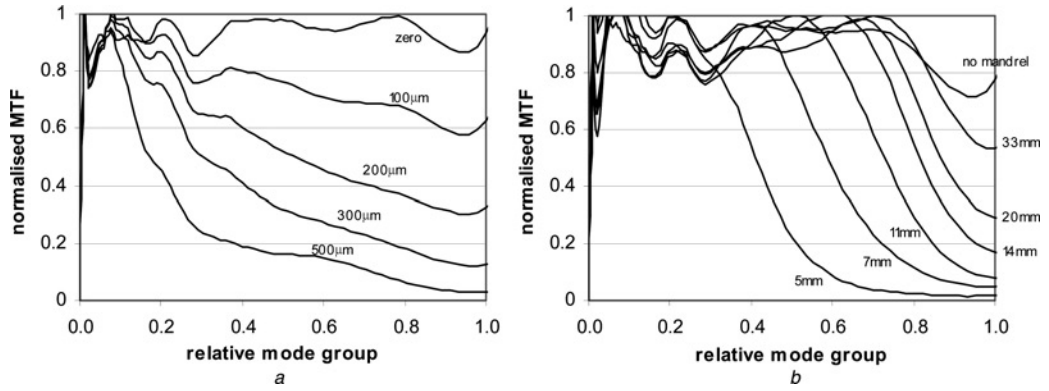


**Figure 6** *Mode transfer functions*

*a* Longitudinal filter, against air gap
*b* Mandrel-wrap filter against mandrel diameter

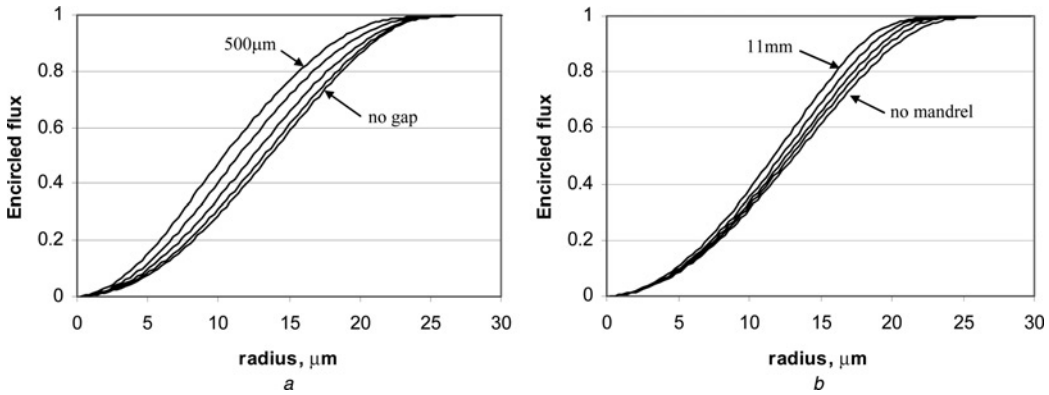


**Figure 7** *Encircled flux*

*a* Longitudinal filter against air gaps of 0, 100, 200, 300, 500 $\mu$m
*b* Mandrel-wrap filter against mandrel diameters of no mandrel, 33, 20, 14, 11 mm

position, but converge towards the edge of the core. In contrast, the mandrel-wrap mode filter predominantly affects the higher-order modes, towards the core boundary, which are progressively attenuated as the bend diameter is reduced. By using a combination of the two types of filter, it is possible to produce a range of encircled flux profiles to suit particular standards requirements.

## 4 Wavelength sensitivity

Many commercial dual-wavelength LAN testers employ a means of combining the output from two sources at different wavelengths into common output connector. This arrangement clearly speeds up the measurement process and assists in automation, but it is also important to

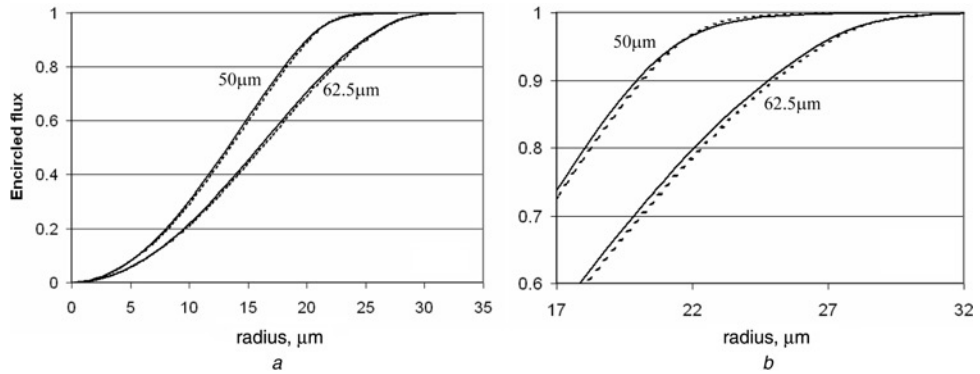


**Figure 8** *Measured encircled flux at 850 nm (dotted) and 1300 nm (solid) for 50 and 62.5 μm mode control devices*

*a* Full curve
*b* Magnified view


*IET Optoelectron.*, 2008, Vol. 2, No. 5, pp. 175–181

doi: 10.1049/iet-opt:20070084

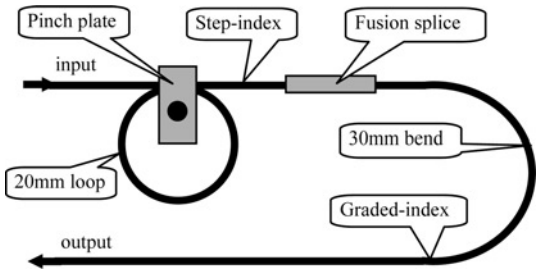


**Figure 9** *Schematic of mode controller*

**Figure 10** *Photograph of ruggedised mode controller*

achieve standards compliance at both wavelengths. To test the wavelength sensitivity of the mode control techniques described above, two devices were assembled with 50 and 62.5 μm output fibres, each comprising a point-load mode scrambler and a mandrel-wrap mode filter of one-half turn of 30 mm diameter. The encircled flux was then measured at 850 and 1300 nm and the results are shown in Fig. 8. The encircled flux at 1300 nm is slightly to the left of that at 850 nm for most of the radius, and also that the two curves cross over at a position near to the core boundary, at about 22 μm radius for the 50 μm fibre. It can be shown [16] from theoretical Laguerre–Gauss solutions of parabolic-index fibres that this behaviour may be expected and is due to the occurrence of a slightly longer evanescent tail in the cladding at 1300 nm.

## 5 Application of mode control

A practical mode controller was built, consisting of a point-load mode scrambler in tandem with a mandrel-wrap mode filter, shown schematically in Fig. 9. The step-index input fibre is formed into a 20 mm diameter loop and pressure applied to the crossover points of the fibre by means of a pinch plate. The step-index fibre was spliced to a graded-index output fibre and was formed into a single half-turn of ~30 mm diameter. By means of adjusting the pressure on the pinch plate and the diameter of the bend in the graded-index fibre, the output modal distribution was adjusted to comply with the IEC/ISO14763-3 standard. Fig. 10 shows a fully ruggedised style of the mode controller for field use.

To test the performance of the mode controller, a concatenated link of 50 μm patchcords was assembled,

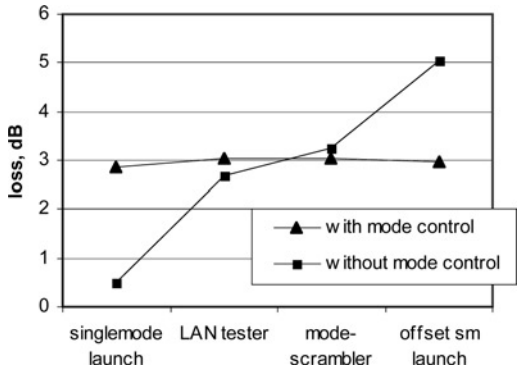


**Figure 11** *Insertion loss of eleven concatenated patchcords*

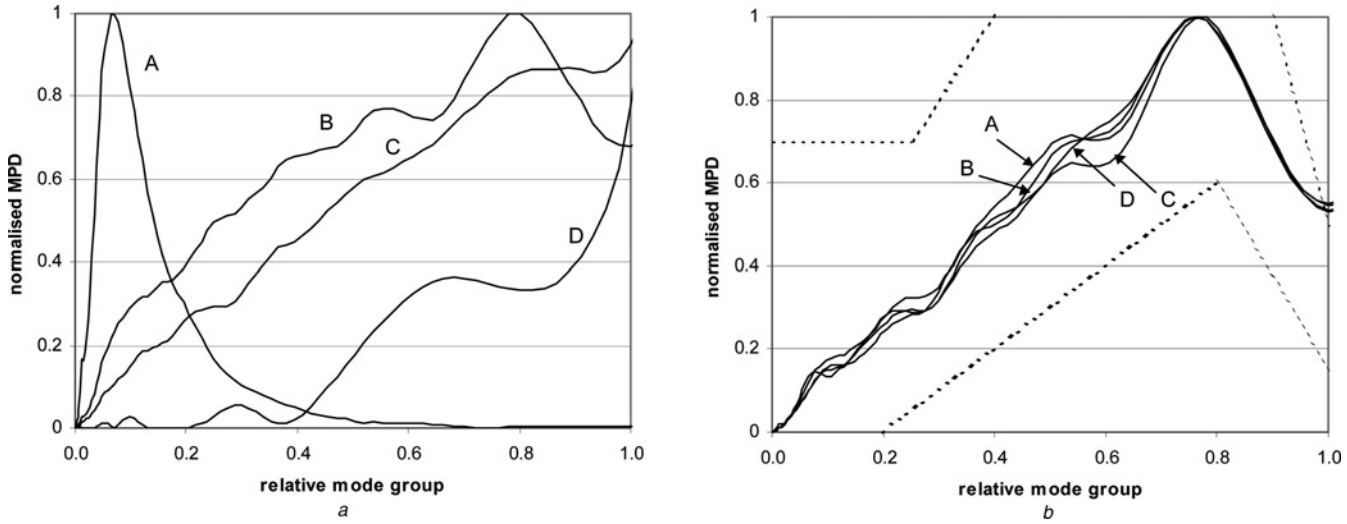


**Figure 12** *Measured MPDs, (a) direct from source, (b) after mode controller. A: singlemode launch, B: LAN tester, C: mode-scrambler, D: offset singlemode launch. The dotted lines show the ISO/IEC14763-3 MPD template*

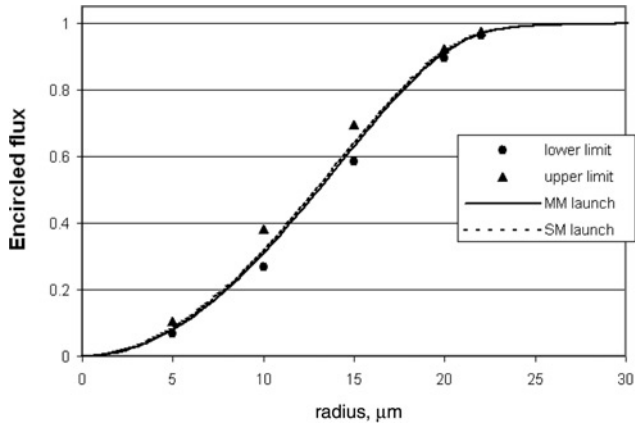


**Figure 13** *Measured encircled flux from mode controller and the encircled flux template from draft IEC61280-4-1*

consisting of 3 m fibre lengths and a mixture of ST, SC and FC connectors. The insertion loss of the link was measured using a variety of light sources, including a single-mode launch, a commercial LAN tester, a mode scrambler and an offset single-mode launch. The loss values, shown in Fig. 11, vary from 0.5 dB, for the single-mode launch, to 5.1 dB for the offset launch. The experiment was then repeated with the mode control device positioned, in turn, between each source and the link under test. The measured range of losses was reduced from 4.6 dB, without the mode controller, to 0.2 dB with it, indicating a great improvement in reproducibility. The MPD of each of the sources was then measured, shown in Fig. 12*a*, and also the MPD after the mode controller was fitted, shown in Fig. 12*b*. The areas marked by dotted lines in the top corners, and lower centre, correspond to the MPD template specified in the ISO/IEC14763-3 link testing standard.

IEC standard IEC61280-4-1 [17] specifies the launch conditions in terms of upper and lower tolerances of the encircled flux distribution at different radial positions. By using the point-load mode scrambler in tandem with a mandrel-wrap mode filter, it was possible to produce an encircled flux profile to comply with the standard, shown in Fig. 13. Both a single-mode launch and a multimode launch were tested, demonstrating the insensitivity of the device to the launched distribution.

## 6 Summary

The use of mode control techniques to enable commercial test equipment to achieve compliance with international standards has been described. A novel point-load mode scrambler operating in series with air gap, and mandrel-wrap, mode filters was shown to be able to produce a variety of MPDs and encircled flux profiles. In particular, compliance with launch requirements in link testing standards was achieved. Improvement in the reproducibility of insertion loss measurements on concatenated patchcords was demonstrated by inserting the device between a variety of test sources and the fibre under test. The mode control device showed a very low sensitivity to launched distribution and was able to achieve standards compliance at both 850 and 1300 nm.

## 7 References

[1] ISO/IEC14763-3: 'Information technology – implementation and operation of customer premises cabling – part 3: testing of optical fibre cabling', 2006

[2] IEEE 802.3-2005: 'Information technology – telecommunication & information exchange between systems – local and metropolitan area networks – specific requirements, Part 3. Carrier sense multiple access with collision detection (CSMA/CD) access method and physical layer specifications'. Amendment 802.3aq, 2006

[3] IEC PAS61300-3-43: 'Examinations and measurements – modal distribution measurement for fibre optic sources'. (2006, 1st edn.)

[4] TIA/EIAFOTP-455-203: 'Launched power distribution measurement procedure for graded-index multimode fiber transmitters'. June 2001

[5] TOKUDA M., SEIKAI S., YOSHIDA K., UCHIDA N.: 'Measurement of baseband frequency response of multimode fibre by using a new type of mode scrambler', *Electron. Lett.*, 1977, **13**, (5), pp. 146–147

[6] SCHLAGER J.B., ROSE A.H.: 'Annealed optical fibre mode scrambler', *Electron. Lett.*, 2001, **37**, (1), pp. 9–10

[7] IKEDA M., MURAKAMI Y., KITAYAMA K.: 'Mode scrambler for optical fibers', *Appl. Opt.*, 1977, **16**, (4), pp. 1045–1049

[8] SU L., CHIANG K.S., LU C.: 'Microbend-induced mode coupling in a graded-index multimode fiber', *Appl. Opt.*, 2005, **44**, (34), pp. 7394–7402

[9] IKEDA M., SUGIMURA A., IKEGAMI T.: 'Multimode optical fibers: steady state mode exciter', *Appl. Opt.*, 1976, **15**, (9), pp. 2116–2121

[10] RADDATZ L., WHITE I.H., CUNNINGHAM D.G., NOWELL M.C.: 'An experimental and theoretical study of the offset launch technique for the enhancement of the bandwidth of multimode fiber links', *IEEE J. Lightwave Technol.*, 1998, **16**, (3), pp. 324–331

[11] YAMASHITA K., KOYAMADA Y., HATANO Y.: 'Launching condition dependence of bandwidth in graded-index multimode fibers fabricated by MCVD or VAD method', *IEEE J. Lightwave Technol.*, 1985, **3**, (3), pp. 601–607



doi: 10.1049/iet-opt:20070084

[12] YOUNG W.C., BUDYNAS R.G.: 'Roark's formulas formulas for stress and strain' (McGraw-Hill, 2002, 7th edn.)

[13] OLSHANSKY R.: 'Distortion losses in cabled optical fibers', *Appl. Opt.*, 1975, **14**, (1), pp. 20–21

[14] MARCUSE D.: 'Coupled mode theory of round optical fibers', *Bell Syst. Tech. J.*, 1973, **52**, (6), pp. 817–842

[15] BOROWSKI E.J., BORWEIN J.M.: 'Dictionary of mathematics', (Harper Collins, 1989, 1st edn.)

[16] HALLAM A.G.: 'Mode control in multimode fibre and its applications', PhD thesis, Aston University, 2007

[17] IEC 61280-4-1: 'Installed cable plant – multimode attenuation measurement'. Committee Draft, 2007